A Novel Tactile Display for Softness and Texture Rendering in Tele-Operation Tasks

Matteo Bianchi[1*], Mattia Poggiani[2*], Alessandro Serio[2] and Antonio Bicchi[1]

***Abstract*— Softness and texture high-frequency information represent fundamental haptic properties for every day life activities and environment tactual exploration. While several displays have been produced to convey either softness or high-frequency information, there is no or little evidence of systems that are able to reproduce both these properties in an integrated fashion. This aspect is especially crucial in medical tele-operated procedures, where roughness and stiffness of human tissues are both important to correctly identify given pathologies through palpation (e.g. in tele-dermatology). This work presents a fabric yielding display (FYD-pad), a fabric-based tactile display for softness and texture rendering. The system exploits the control of two motors to modify both the stretching state of the elastic fabric for softness rendering and to convey texture information on the basis of accelerometer-based data. At the same time, the measurement of the contact area can be used to control remote or virtual robots. In this paper, we discuss the architecture of FYD-pad and the techniques used for softness and texture reproduction as well as for synthesizing probe-surface interactions from real data. Tele-operation examples and preliminary experiments with humans are reported, which show the effectiveness of the device in delivering both softness and texture information.**

I. Introduction

Softness and texture are two fundamental types of information that shape our haptic perception of the external world.

Softness represents the subjective counterpart of object compliance and plays a crucial role in everyday life tasks [1], since it provides fast perceptual cues strictly related to the semantic representation of objects [2]. At the same time, texture information, i.e. the high-frequency information relying on surface irregularities, contacts and acceleration signals, was defined as one of the primary means of object exploration given its importance in determining how humans interact with the environment [3].

It is not hence surprising that a lot of effort has been devoted to investigate and artificially reproduce these haptic stimuli through tactile/kinaesthetic devices that can increase the immersiveness of the interaction in virtual or remotely tele-operated scenarios. Several softness displays were proposed [4] based on different actuation methods, ranging from electrorheological and magnetorehological fluids, to pneumatic arrays and skin-stretch-based mechanisms [5], [6], [7], [8]. Among these techniques, contact area control was proven to be an effective manner to convey tactile information involved in softness discrimination and it was used to drive the realization of softness displays [9], [10], [11], [12], [13], [14].

Fig. 1: A subject fingertip interacting with the FYD-pad.

Regarding texture rendering, it was demonstrated that the inclusion of high-frequency contact information significantly increases the realism of haptic experience [15]. However, a reliable representation of surface texture still remains challenging, e.g. due to the difficulties in recording high-frequency interactions with the surface or the lack of accurate dynamic models [16]. Different technological systems have been proposed to try to overcome these limitations that affect common haptic displays. For example, physics-based haptic devices model high-frequency contact information using tools such as fractal simulation of object surfaces [17] or Fourier series models of recorded topographical surface data [18]. Other works focus on the sensation elicited in users to drive the design of haptic systems [19], [20].

Data-driven haptic rendering represents an alternative approach that exploits high-frequency data arisen from the interactions with real objects to design virtual textures or to enhance the realism of master-slave tele-operation tasks, especially in medical applications. Such an approach was pioneered in [21], where a voice-coil actuator was used to superimpose acceleration waveforms recorded at the slave robot. This method was further refined and developed in successive works: e.g. the *VerroTouch* system for robot-assisted surgery [22], which filtered and amplified the two measured accelerations at the slave side and used a pair of vibration actuators to re-create these acceleration profiles at the fingertips of the surgeon.

In [23] authors presented a sensorized hand-held tool to capture the feel of a given texture and linear predictive coding to distil this raw haptic information into a database of frequency-domain texture models. These models were then rendered in real time through a Wacom tablet and a stylus equipped with small voice coil actuators.

[1] M. Bianchi and A. Bicchi are with Centro di Ricerca "E. Piaggio", Università di Pisa, Largo L. Lazzarino, 1, 56100 Pisa, Italy and with the Department of Advanced Robotics, Istituto Italiano di Tecnologia, via Morego, 30, 16163 Genova, Italy. {m.bianchi} at iit.it {bicchi} at centropiaggio.unipi.it

[2] M. Poggiani and A. Serio are with Centro di Ricerca "E. Piaggio", Università di Pisa, Largo L. Lazzarino, 1, 56100 Pisa, Italy. {mattiapoggiani} at gmail.com, {a.serio} at centropiaggio.unipi.it

[*] These authors contributed equally to this work.

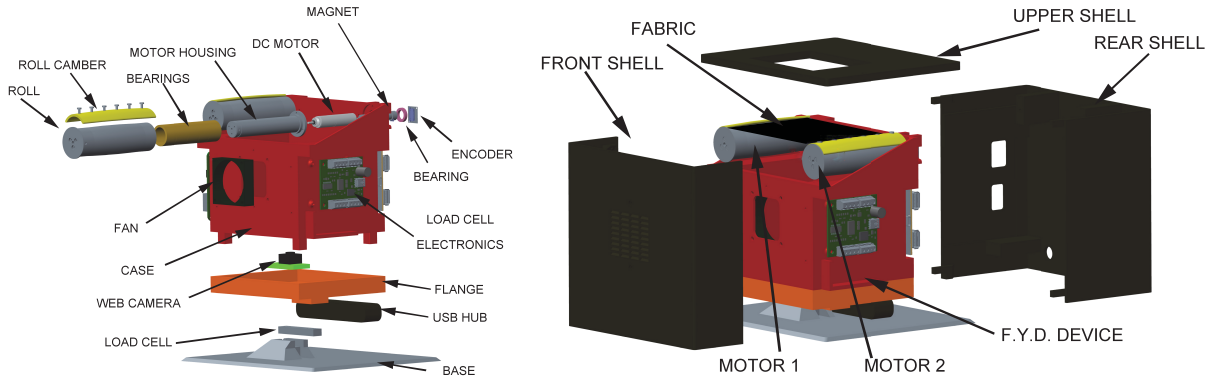

Fig. 2: Exploded drawing of the FYD-pad.

While these methods consider tool-mediated vibrations and texture rendering, other works deal with bare finger interactions. In [24] an electrostatic tactile display was presented, which was based on a thin conductive film slider with stator electrodes exciting electrostatic forces, while the users experienced tactile texture sensations by moving the slider with their fingers. In [25] authors presented the design and evaluation of a high fidelity surface haptic device, where users slid their finger along a glass plate and friction was controlled via the amplitude modulation of ultrasonic vibrations of the plate. This system was proven to be able to reproduce fine textures directly on the user's bare finger.

Despite the technological effort for rendering one of the two haptic stimuli (softness or texture), there is little evidence of fully integrated tactile devices able to reproduce both these types of information. For example, in [26] a wearable, ungrounded haptic display to present the gravity sensation of a virtual object and shearing stress was described, even if the correct integration of softness and texture cues was not addressed. To the best of our knowledge, the only attempt to convey both these tactile feelings on one device was in [14], where the mechanism for softness presentation reported in [9] was integrated with the electrostatic tactile display described in [24]. However the results were very preliminary and experiments on the perception elicited in humans lack. Furthermore, the applicability in tele-operation tasks of this system is limited, for example because of the softness control of the contact area that acts on the vertical direction. This fact is hardly compatible with the constraints of the workspace, which are especially important in robot-assisted minimally invasive surgery [27].

Indeed, surgery and medical tele-applications and training represent the ideal field of application of an integrated display for texture and softness rendering. For example, let think about the *tele–dermatology* project [28] carried out at Stanford University, whose goal was to deliver tactile images of the human skin to a dermatologist at a remote location, in real time. In this case, to properly make a diagnosis, dermatologists need information about both the skin texture and the mechanical properties of lesions on the patients skin. Indeed, the roughness of pre-cancerous or weather-damaged skin is greater than the roughness exhibited by normal skin, while the profile and stiffness of the underlying tissue may give suggestions on the nature of a skin disease.

To fulfill tele-operation requirements and increase the immersiveness of the haptic experience, we propose FYD (Fabric Yielding Display) - pad (see fig. 1), a fabric-based fully integrated device able to render both texture and softness information, that can be used as a potentially useful training tool for physicians and with possible applications in robotic tele-operation. The system exploits the control of two motors to modify both the stretching state of the elastic fabric to render a given softness level (as discussed in our previous works [11], [12], [29]) and to convey texture information on the basis of accelerometer-based data (as reported in [22], [16]). At the same time, the measurement of user finger position can be used to control remote or virtual robots. In this paper, we discuss the architecture of FYD-pad and the techniques used for softness and texture reproduction as well as for synthesizing probe-surface interactions from data recorded from real tool-mediated interactions. Examples of tele-operation tasks are also discussed. Notice that in this particular work we do not consider "tele-presentation" task, which implies that both measurement of remote haptic information and its rendering at the master site are performed in real-time.

Preliminary experiments with humans interacting with their bare fingers with the fabric surface show the effectiveness of the here proposed device in delivering both softness and texture information.

II. System Architecture

FYD - pad exploits an elastic fabric to jointly convey softness and texture information, by performing digital texture rendering through Pulse Width Modulation (PWM) of two DC motors, on the basis of accelerometer data and synthesized probe-surface interactions [16], while softness information is rendered by modulating the stretching state of the fabric as in [11], [12] (as it will be further discussed in the next Sections). At the same time, the dynamic movement of the user finger on the elastic tissue allows to remotely control a robot linked through an informatic network, by tracking finger location on the fabric and measuring force and indentation. Although FYD-pad architecture is inspired by works in [11], [12], there are some important differences w.r.t. previous displays that can be roughly summarized as follows: (i) implementation of texture rendering for soft materials, in addition to the reproduction of different softness

levels; (ii) direct measurement of indentation; (iii) a novel algorithm to estimate the centroid of the contact area to use the FYD-pad as the master joystick for tele-operation tasks; (iv) wireless and wired communication for the control of virtual and/or remote robots in tele-operation applications. Moreover, as it will be discussed in more details in the following sections, to avoid the system becomes slow, FYD-pad software was organized in multiple threads of executions, each one devoted to a FYD-pad functionality with its own operating frequency.

A. Mechanical Description

FYD-pad uses a layer of isotropic elastic fabric, Superb-iflex HN by Mectex S.P.A (Erba, Como, Italy) with good resistance to traction, whose extremities are connected to two rollers, each of them is independently moved by a pulley placed on a motor shaft. The architecture is inspired by [11], [12]: more specifically, we used DC Maxon Motor REmax [11]. The motors are inserted into the rollers, while a custom made electronic board by QB Robotics® (PSoC-based electronic board) controls motor positions on the basis of the readings of two absolute magnetic encoders.

An exploded drawing of the system is shown in fig. 2. The dimensions of FYD-pad are 140 mm (height) × 150 mm (length) × 120 mm (width), in order to provide a large enough workspace to enable a reliable tele-control of slave robots. However, since the architecture is fully scalable, they can be easily reduced.

FYD-pad is also capable to on-line detect finger position, by computing both (i) the centroid of the contact area (in the x-y plane) and (ii) the indentation of the user's finger on the fabric surface (along z-axis, see fig. 3). More specifically, to get objective (i) we placed just beneath the fabric (100 mm) (see fig. 2) a web camera (Microsoft "LifeCam HD–3000" with a resolution of 640 × 480 @ 30 fps), with vertical focal axis. The 30 fps frame rate allows to perform a good tracking with finger movement speeds up to 40 mm/s (see Subsection III-B). For objective (ii), we placed three contact-less infrared Sharp® analog distance sensors (GP2Y0A41SK0F) with detection range 4-30 cm on the base of the device (at 100 mm of distance from the fabric) in a triangular configuration, as reported in fig.3 and explained in Subsection II-B. FYD-pad is also endowed with a load cell (Micro Load Cell, 0 to 780 g, - CZL616C - from Phidgets (Calgary, AB – Canada)) placed at the base of the device, to record the normal force exerted by the finger interacting with the fabric and a USB hub attached at the flange of the device, which hosts the USB ports from webcam, load cell and QB electronics and which is connected to a pcDuino® board (mounted on the rear of the case), where the estimation algorithms we used to achieve goals (i) and (ii) are also implemented.

B. Sensing Part

In this Subsection we discuss the algorithms used to estimate the centroid of the contact area and the indentation of user finger interacting with the fabric. Validation of the here described methods is also discussed.

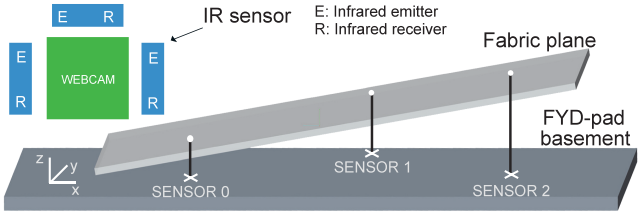

Fig. 3: Indentation estimation scheme and sensor placement (top view).

1) Centroid Estimation: The finger detection algorithm is based on the images captured with the webcam (x-y plane, see fig. 4) and uses the OpenCV® computer vision library. The algorithm runs every 100 milliseconds, with contrast level and brightness level set to maximum. We used intensity threshold (heuristically found) to determine contact area [11]. However, as opposed to [11], we identified the contact area of the finger since it appears darker than the background, due to the shadow produced by the finger on the webcam against the external light.

We defined a region of interest (ROI, 160 px × 120 px) on the basis of the workspace area on the fabric (100 mm × 70 mm): these dimensions were chosen to correctly enable synthesized texture rendering as described in Subsection III-C and for possible tele-operation actions with remote robots. The images from the webcam were then converted using gray scale levels. We heuristically set the threshold to 150, i.e. only pixels darker than the threshold value were recognized as belonging to the finger [1] (only for visualization purposes, the resulting binary image were inverted in order to have the pixels belonging to the finger area displayed as white).

Once the finger area was computed (knowing the camera resolution and the number of white pixels), the centroid can be obtained assuming a Gaussian distribution for the pixels belonging to the contact area, starting from the pixel with minimum intensity, i.e. $value_{min}$, and associating a weight depending on the distance in terms of intensity with respect to $value_{min}$ to the other pixels.

The weight k can be computed for each pixel as $k = e^{\frac{-(x-\mu)^2}{2\sigma^2}}$, where $\mu = value_{min}$ and $\sigma = \frac{(value_{max} - value_{min})}{\beta}$, with β heuristically set to 5. A weighted average of all the pixels in the finger image identifies the pixel corresponding to finger centroid. The validation of this algorithm can be obtained in a preliminary manner from the results reported in Subsection IV-B, which show the effectiveness of tele-operation control, and in Subsection IV-A, where the computation of the velocity is based on centroid position differentiation for rendering synthesized textures and for human experiments. However, a thorough validation will be performed in future works. In order to enable proper tele-operation tasks, we mapped the ROI of finger image to the robot end-effector workspace using a 1:1 scale.

C. Indentation estimation

The indentation estimation, i.e. how much the finger indents the fabric surface, can be obtained by measuring

[1]Notice that pixels value belong to range 0-255, where 0 is associated to a black pixel and 255 to a white one.

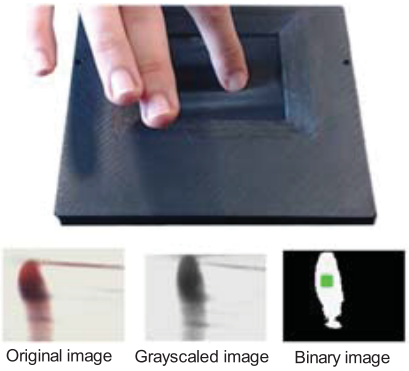

Fig. 4: Example of how the webcam detected finger movement on the fabric.

the distance from structure flange to the indented fabric. To achieve this goal three infrared sensors are heuristically arranged on the base in a triangular configuration in order to minimize IR interferences and to detect points that are always non-collinear (this is important for the estimation procedure, as it is explained in the following lines).

Each sensor gives a voltage value (v) that is inversely proportional to the measured distance (d) from the fabric (in millimeters). The following 5th order linear interpolation ($R^2 = 0.9987$) was used

$$d = -4.6327v^5 + 39.954v^4 - 133.8297v^3 + 220.8604v^2 - 188.5623v + 79.0712 \quad (1)$$

To estimate finger indentation we compute the distance of the plane passing from the 3D points detected by sensors from the base. Indeed, on the basis of geometrical considerations only one plane can pass through three non collinear points. Fig. 3 shows in light gray what is the plane generated from the three 3D points. IR sensors are placed at fixed and pre-known x and y coordinates from the center of the fabric area. Sensed distances, representing the z coordinates of three 3D points, are subtracted to the measured base-fabric distance when no finger is touching ($\bar{z}$). An indentation estimation can be found computing δ from the following plane equation

$$e_1(44y+132) - 1320\delta - e_0(30x+22y-594) + e_2(30x-22y+594) == 0 \quad (2)$$

where $e_i = z_i - \bar{z}_i$ with $i = 0,1,2$ referring to each IR sensor and x and y represent the finger centroid position. To validate this result fabric indentation made by the servo-motor indenter of the characterization system described in [12] has been compared to the plan estimation obtained using distance sensors. The planar approximation is a valid choice ($RMSE = 2.88mm$) if indentation belonged to range 0-50 mm, which is inside the average range of indentation observed during tele-operation tasks and tests with humans.

Notice that the estimation completely relies on distance measurements from IR sensors and additional information on the fabric (e.g. stiffness) is not required to get the estimated indentation.

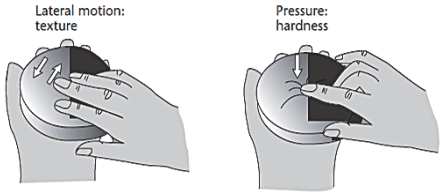

Fig. 5: Exploratory procedures generally used by people to perceive roughness and softness (courtesy of [2]).

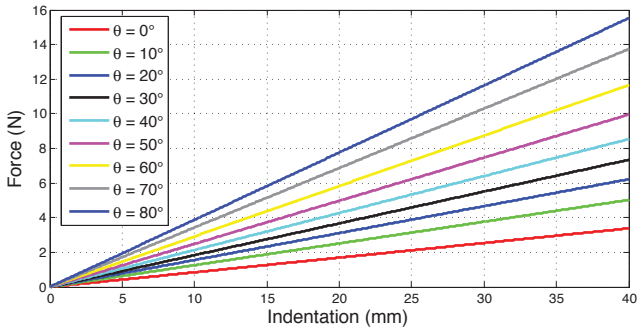

Fig. 6: Force-indentation curves of FYD-pad at different motor positions (θ). $\theta = 0$ is the rest position of the motors.

III. Haptic Rendering

The driving idea for haptic rendering in FYD-pad is the concept of the Exploratory Procedures (EPs) first introduced in [30] to indicate stereotyped hand motions characteristic of human haptic exploration. The main finding was that the EPs used by subjects were chosen on the basis of the haptic property to be determined and were optimal for such a property [30], [31]. More specifically it was demonstrated that lateral motion is optimal for texture exploration while pressure for softness exploration, see fig. 5. With this as motivation, the FYD-pad was built in order to independently enable such EPs in users: lateral motion with negligible pressure for texture discrimination and pressure for softness.

FYD-pad was also endowed with an additional functionality: by suitably tracking the finger position, it is possible to use the system to tele-operate a virtual finger and a remote robotic end-effector.

A. Softness Rendering

A given level of softness is associated to a stretching state of the fabric and it can be achieved by suitably controlling the position of the two motors as described in [12]. The system was characterized using the characterization system previously described. Characterization curves were linear ($R^2 > 0.932$), as shown in fig. 6. The range of reproducible stiffness levels is 0.262-1.04 N/mm: no significant differences were observed in stiffness characterization in the workspace area.

B. Texture Rendering

We followed a data driven approach for texture rendering as in the analog approach described in [22]: accelerations signals were recorded, filtered and then amplified to drive the actuator that will render high-frequency information. Indeed, signals must be first filtered in order to convey the best haptic stimuli to Pacinian corpuscles, whose sensitive band is from 20 to 1000 Hz [32] . Compared with [22],

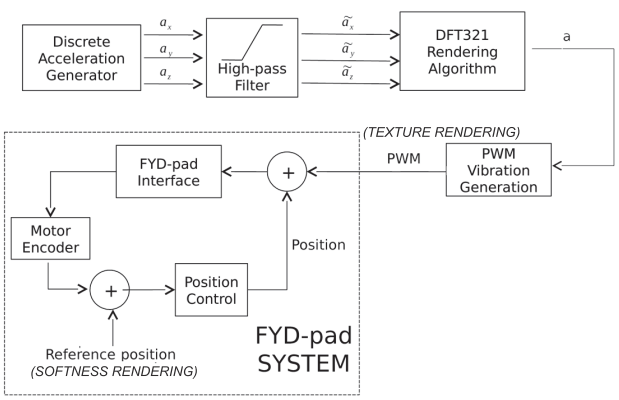

Fig. 7: Control scheme for FYD-pad softness and texture rendering.

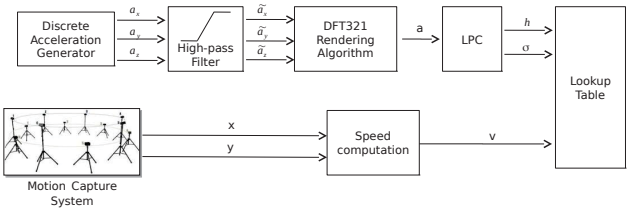

Fig. 8: The LPC-based texture modelling system.

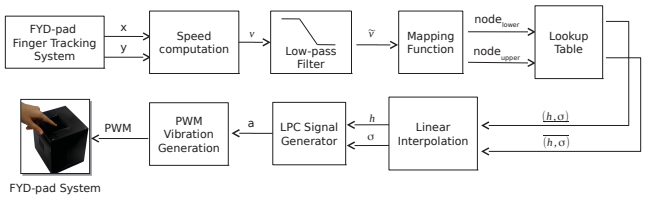

Fig. 9: The LPC-based texture rendering system.

we adopted a different filter bandwidth, individuated through acceleration data preliminary acquired from different rough compliant materials (such as sponges, etc...) We chose a bandwidth of interest around 190 Hz with lower and upper limits respectively around 165 Hz and 220 Hz.

In order to implement vibrotactile texture rendering to the discrete domain to be used with FYD-pad, we controlled the two FYD-pad motors using Pulse Width Modulation (PWM) technique with a duty cycle that varied according to the vibration to reproduce on the fabric (see scheme on fig. 7). This control was summed to the internal position control ($input_{POSITION}$), which was used to maintain a fixed stiffness on the tissue (in our case it is simply based on the look-up table obtained from fabric characterization), that was

$$input_{PWM} = input_{POSITION} + input_{VIBRATION} \tag{3}$$

The input vibration duty cycle ($input_{VIBRATION}$) was computed according to a digital time signal obtained using a specific rendering algorithm. Since human perception is not sensitive to the direction of vibration and given the problem to reduce the 3-axis accelerometer signals into a signal driving a one Degree of Freedom (DoF) motor, we chose the approach that used a frequency-based solution called DFT321 (because it was based on discrete-time Fourier transform and mapped the three-dimensional signal of acceleration to a monodimensional one) [33] [23]. This approach was proven to provide the best results in terms of transparency of the reproduced high-frequency information versus the measured one.

In order to synthesize an artificial texture close to the real one, we captured real texture acceleration data at different material scanning speeds. We constructed a 3D-printed plastic tip with a support for a 3-axis digital $\pm 5g$ accelerometer with frequency@1kHz [16]. The position of this tip in space was tracked using the Phase Space motion capture system, which can measure the position in space of active LED markers (the amount of static marker jitter is inferior than 0.5 mm, usually 0.1 mm and the acquisition frequency is 400 Hz). Eight markers were placed on the tip, to ensure robustness to the occasional loss of markers. From the position measurements, velocity was estimated by discrete-time derivation. We heuristically chose to acquire data with different scanning velocities, from 10 to 40 mm/s at steps of 10 mm/s, and we considered the acceleration acquisition valid only if the experimenter performing material scanning did not deviated more than 5 mm/s away for the target speeds. Accelerometer measurements were used to develop a transfer-function model based on the DFT321 monodimensional signal according to linear predictive coding (LPC) [23], which takes into account different scanning speeds. We stored the results in a lookup table at the proper speed indices; the table is composed by the LPC recursive coefficients $\vec{h}$ and the power of the residual signal σ^2. The vector of filter coefficients $\vec{h}$ was defined as the optimal vector that minimized the residual between the DFT321 rendered acceleration data vector (a) and the prediction vector $\widehat{a}$ which was defined at time step k as

$$\widehat{a}(k) = \vec{h}^T \vec{a}(k-1) \tag{4}$$

We found that a filter coefficient vector of 200 items was able to both reduce the residual and to not introduce delay in computation while used real-time. The σ^2 power of residual signal was computed as the average squared magnitude of the individual signal elements (in the range of .001 and .0001). An off-line data elaboration generated a file with $\vec{h}$ and σ^2 coefficients that were used in FYD-pad system for virtual texture rendering. The whole acquisition procedure is summarized in fig. 8.

To render material roughness on FYD-pad device, we referred to the scheme proposed in fig. 9. Fingertip position on the FYD-pad fabric is computed as reported in II-B. The raw position data were used to compute fingertip speed using an on-line time derivation method. A 10 Hz low-pass filter was applied to speed values. Then, we retrieved data from the lookup table corresponding to the two closest entries in speed within the table. These two couples of $(\vec{h}, \sigma^2)$ data were linearly interpolated to obtain current $\vec{h}$ LPC coefficients vector and σ^2 error variance. A LPC signal generator implemented the following equation, which shows how to obtain at time step k an updated synthesized acceleration value ($a(k)$) in order to generate an appropriate acceleration waveform (vector $\vec{a}$) using LPC model parameters and accelerations obtained at previous steps:

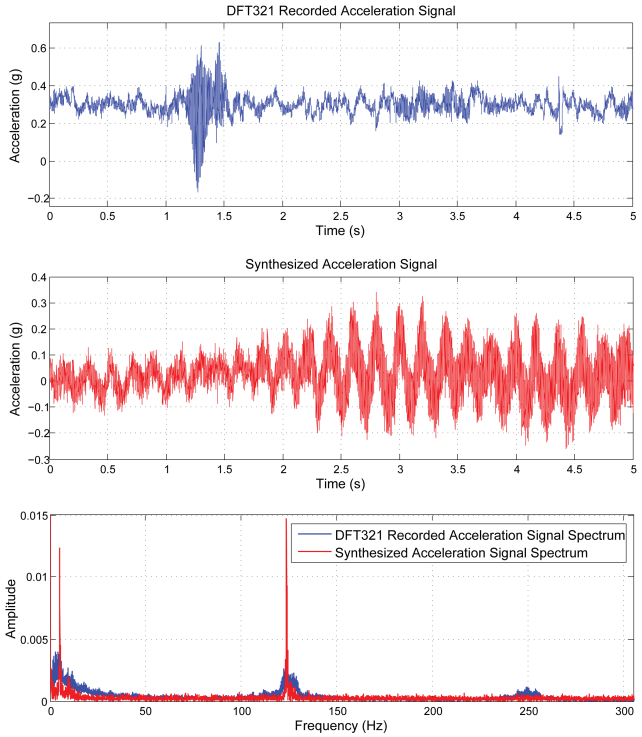

Fig. 10: Time and frequency domain views of both a monodimensional real recorded acceleration signal obtained using DFT321 procedure and a synthesized acceleration signal obtained using LPC technique. Even if the two signals are temporally distinct, they have similar spectra.

$$a(k) = e(k) + \vec{h}^T \vec{a}(k-1) \tag{5}$$

where $e(k)$ is a white noise signal with a Gaussian distribution of amplitudes and variance equal to signal power σ^2, since we are considering zero-mean signal. The synthesized acceleration signal was used to drive FYD-pad motors at a 1 KHz frequency using the texture rendering PWM-based technique exposed in this section. The strength of vibrations on fabric could be adjusted for each texture according to user preference. We preliminarily chose a gain of 1 (i.e. final motor vibration corresponded to the value computed by LPC rendering methodology) and we will investigate it in future works. For further details on this rendering technique, please refer to [23].

C. Tele-Operation Task

The tele-operation task was based on contact area detection of the user finger on FYD-pad fabric. More specifically, the dynamic movement of the user finger on the elastic tissue allowed to remotely control a virtual or real robot linked through an informatic network, by tracking centroid location on the fabric. The device could be easily interfaced with different manipulators since it could communicate with external robots using a protocol based on packet exchange, with both wired and wireless networks. The haptic device acted as the tele-operation master and the detected position of the finger was sent to the slave robot, which implemented an internal position control to drive its end effector to the desired position, thus minimizing error. The finger detection procedure to extract centroid information was based on the processing of images captured from the web camera placed on the base of the FYD-pad device, as described in section II-B.1. While the position on the fabric was computed using finger centroid, the information on the third spatial coordinate, i.e. the finger indentation, is computed reading the three analog contact-less distance sensors and performing a plane-based algorithm that gave back the estimated indentation of the finger centroid.

IV. Experimental Validation

In this section we will show some examples of the rendering capabilities of the device, in terms of reliability of the haptic stimuli to be conveyed. We prepared silicone specimens with different roughness and softness and we applied the methods described in Section III to render them in terms of these two haptic information types. We will also report the performance of the system in terms of the master in a master-slave configuration with virtual or real end-effectors in different environmental configurations. Finally we will report some preliminary experiments with humans to show the effectiveness of FYD-Pad in providing realistic haptic stimuli.

A. Specimen Characterization and Rendering

We realized four types of silicone specimens, hereinafter referred to as SS, to properly validate FYD-pad performances in terms of softness and texture rendering. The specimens were cylinders of radius 17.5 mm and height 10 mm and they were made with a mixture of 50 % SYLGARD 184 silicone elastomer (Dow Corning, USA) with monomer catalyzer rate 1:10 (w/w) and of 50 % SYLGARD 527 with monomer catalyzer rate 1:1 (w/w) in SS1 and SS2 specimens, while SS3 and SS4 were made with SYLGARD 184 with monomer catalyzer rate 1:40 (w/w). The specimens to be characterized in softness were placed under the system described in [12]: as the finger-shaped indenter pushed against the specimens, we recorded force and indentation. In this manner we obtained $F(\delta)$ curves for SS1, SS2, SS3 and SS4. Force-indentation curves were interpolated using a linear approximation ($R^2 > 0.924$), that is $F(\delta) = \lambda\delta$. The two levels of softness we founded were 0.88 N/mm (S1) for SS1 and SS2, 0.39 N/mm (S2) for SS3 and SS4. The couples of silicones with the same softness presented two different levels of roughness, that is SS1 and SS3 have R1 roughness level while SS2 and SS4 have R2 roughness level. Roughness on specimens surface was obtained making rectangular gratings with variable spatial periods (ridge plus groove width): in particular, R1 level had a spatial period of 3.90 mm, while R2 level had a spatial period of 2.15 mm. In both levels ridge width was 90% of spatial period while groove width was the remaining 10%. Using the procedure described in III-B, we were able to synthesize acceleration and velocity data and to build a lookup table for each of the four specimens to be used in FYD-pad texture rendering. In the rendering phase, we created an acceleration signal to simulate contact with virtual texture. The method is summarized in fig.9. Results are shown in terms of time and frequency correlation between the accelerations perceived on FYD-pad fabric along the fabric stretching direction

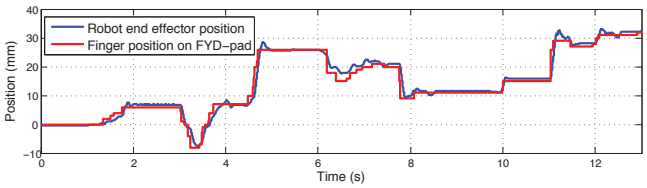

Fig. 11: Y coordinate evolution during a tapping experiment on FYD-pad haptic device and relative tracking on the robot connected by wired network.

(using DFT321 rendering algorithm to drive motors) and the acceleration signal along the tip motion axis while scanning specimens, taking into account the transformation between the two systems of reference. Before computing correlation, acceleration signals were filtered using a digital high-pass filter with 10 Hz as a cut-off frequency to remove low frequency tip motion. The tip used to acquire acceleration on SS1 was the same described in III-B, used to capture texture acceleration data. In terms of performances indexes, time correlation results had a value of 0.263, while the correlation in frequency is 0.681 (see fig. 10). These results show that texture performances are comparable with those obtained in literature (see e.g. [22]).

These results, although encouraging, can be improved, for example by using different interpolation methods for multiple texture models other than the linear one we used for this work. Future works will be devoted to further investigate these approaches (see e.g. [34]), thus increasing the quality of roughness rendering.

B. Tele-Operation Performance

To prove tele-operation tasks, the haptic FYD-pad interface was tested using a KUKA® lightweight 7-DoF manipulator as tele-operation slave. Position control was performed acquiring the position data from the finger on FYD-pad fabric sent to the robot through a communication network, while attitude was chosen to remain fixed, so that the robot end effector was always perpendicular to the surface to explore. In these experiments the user moved his finger all along the fabric, while the robot received finger position through network and performed an internal position control to reach the 3D position with its end effector. We tried different trajectories such as circular paths, a Lissajous-like curve and a simple tapping on the fabric. Results are reported in fig. 11: they are positive, despite a slight discrepancy due to the different working frequency for the FYD-pad software and the robot software (10 Hz vs. 1 kHz). We chose as the index used to measure performances the mean absolute position error (MAE), computed for all the three spatial components ($j = x, y, z$) as

$$MAE_j = \frac{1}{n}\sum_{i=1}^{n}|err_i| \tag{6}$$

where err_i indicates the error between master and slave positions on j-th axis and n represents the number of samples. Experiments results show user finger tracking is well performed, since MAE is approximately 3 millimeters on all the trials and all the directions (i.e. a percentage error of 3-4 % with respect to the finger usable area (100 × 70 mm)).

C. Experiments with Humans

To properly characterize FYD-pad performance in terms of its capability in eliciting a correct texture and softness perception, we performed absolute cognition tasks [9]. More specifically, participants were asked to correctly associate the artificial silicone specimens with the real ones. Six right–handed healthy participants (F, Age: 28.38 ± 3.30, mean $\pm$ SD) gave their informed consent to participate to the experiment. No one had any physical limitation which would have affected the experimental outcomes. The experimental procedure was approved by the Ethical Committee of the University of Pisa.

SH1, SH2, SH3 and SH4 were presented three times in a random order to participants and then they were asked to associate them to their physical counterparts SS1, SS2, SS3 and SS4. One rendered specimen was randomly presented at one time. Real specimens were positioned on a white sheet of paper on the desk near the arm stand, so that the participant did not have to do large excursions with the arm. The silicones were posed on numbered circles on the sheet in a random order for each participant. Participants were required to touch with the index of their dominant hand both the artificial and real specimens using the two previously mentioned EPs, i.e. lateral motion and pressure with no constraints on the order of usage. Notice that participants were requested to perform these two EP actions in a completely independent manner: in this manner, any effect of the interaction between softness and texture rendering on the perception of these quantities was minimized. Participants did not have time limitations since they were allowed to touch the silicone specimens and the rendered stimulus and to go back and forth between them as many times as they wanted. Participants wore headphones with white noise, to prevent the usage of any auditory cue.

TABLE I: Confusion Matrix for Absolute Cognition Task.

	SS1	SS2	SS3	SS4	Relative Accuracy
SH1	11	1	5	1	61.1 %
SH2	0	11	4	3	61.1 %
SH3	0	2	12	4	66.7 %
SH4	1	1	1	15	83.3 %

Results of the ranking experiments are shown in Table I, where the artificially reproduced specimens were associated to their physical counterparts. Values on the diagonal express the amount of correct answers. The average cognition rate is 66.8% (chance level of 25%). Such results is comparable with the ones reported in [23] for texture rendering using analogous techniques to synthesize texture and in [10] for softness rendering, which indicate that FYD-pad is able to render for the first time both stiffness and texture information in an effective manner. Future works will be devoted to better characterize the system under a psychophysical point of view and to further investigate such results.

V. Conclusions and Future Works

This paper presents FYD-pad, a tactile device that is able to render both texture and softness information in an integrated manner and be used as a master for tele-operation applications exploiting the information on finger

user position. The system is also able to render synthesized-texture data obtained from real data measurements. For the first time, experiments with humans show the effectiveness of the system to render both types of information, which further validate the quantitative analysis on the rendering techniques we have reported. Future works will be focused on provide a thorough psychophysical validation of the system. The system might be profitably used for medical applications such as medical training, where tissue roughness and softness are two important types of information to be used for the diagnosis.

ACKNOWLEDGMENTS

This work is supported in part by the European Research Council under the Advanced Grant SoftHands "A Theory of Soft Synergies for a New Generation of Artificial Hands" no. ERC-291166, and by the EU FP7 project (no. 601165), "WEARable HAPtics for Humans and Robots (WEARHAP)". Authors would like to thank Edoardo Battaglia for his help in setting up the experiments.

REFERENCES

[1] W. Tiest and A. M. L. Kappers, "Cues for haptic perception of compliance," *Haptics, IEEE Transactions on*, vol. 2, no. 4, pp. 189–199, Oct 2009.

[2] R. L. Klatzky, S. J. Lederman, and D. E. Matula, "Imagined haptic exploration in judgments of object properties." *Journal of experimental psychology: learning, memory, and cognition*, vol. 17, no. 2, p. 314, 1991.

[3] S. J. Lederman and R. L. Klatzky, "Extracting object properties through haptic exploration," *Acta psychologica*, vol. 84, no. 1, pp. 29–40, 1993.

[4] A. Song, J. Liu, and J. Wu, "Softness haptic display device for human-computer interaction," *Human Computer Interaction, InTech*, pp. 257–277, 2008.

[5] C. Mavroidis, C. Pfeiffer, J. Celestino, and Y. Bar-Cohen, "Controlled compliance haptic interface using electrorheological fluids," in *SPIE's 7th Annual International Symposium on Smart Structures and Materials*. International Society for Optics and Photonics, 2000, pp. 300–310.

[6] A. Bicchi, E. P. Scilingo, N. Sgambelluri, and D. De Rossi, "Haptic interfaces based on magnetorheological fluids," in *Proceedings 2th International Conference Eurohaptics 2002*, 2002, pp. 6–11.

[7] G. Moy, C. Wagner, and R. Fearing, "A compliant tactile display for teletaction," in *Robotics and Automation, 2000. Proceedings. ICRA '00. IEEE International Conference on*, vol. 4, 2000, pp. 3409–3415 vol.4.

[8] S. Yazdian, A. J. Doxon, D. E. Johnson, H. Z. Tan, and W. R. Provancher, "Compliance display using a tilting-plate tactile feedback device," in *Haptics Symposium (HAPTICS), 2014 IEEE*. IEEE, 2014, pp. 13–18.

[9] K. Fujita and H. Ohmori, "A new softness display interface by dynamic fingertip contact area control," in *World Multiconf. on Systemics, Cybernetics and Informatics*, Orlando, Florida (USA), July 2001, pp. 78–82.

[10] A. Bicchi, D. E. De Rossi, and E. P. Scilingo, "The role of the contact area spread rate in haptic discrimination of softness," *IEEE trans. on Robotics and Automation*, vol. 16, no. 5, pp. 496–504, October 2000.

[11] M. Bianchi, A. Serio, E. P. Scilingo, and A. Bicchi, "A new fabric-based softness display," in *Proc. IEEE Haptics Symposium*, 2010, pp. 105 –112.

[12] A. Serio, M. Bianchi, and A. Bicchi, "A device for mimicking the contact force/contact area relationship of different materials with applications to softness rendering," in *Intelligent Robots and Systems (IROS), 2013 IEEE/RSJ International Conference on*, Nov 2013, pp. 4484–4490.

[13] M. Bianchi and A. Serio, "Design and characterization of a fabric-based softness display," *Haptics, IEEE Transactions on*, vol. PP, no. 99, pp. 1–1, 2015.

[14] H. Yokota, A. Yamamoto, H. Yamamoto, and T. Higuchi, "Producing softness sensation on an electrostatic texture display for rendering diverse tactile feelings," in *EuroHaptics Conference, 2007 and Symposium on Haptic Interfaces for Virtual Environment and Teleoperator Systems. World Haptics 2007. Second Joint*. IEEE, 2007, pp. 584–585.

[15] W. McMahan, J. Romano, A. Abdul Rahuman, and K. Kuchenbecker, "High frequency acceleration feedback significantly increases the realism of haptically rendered textured surfaces," in *Haptics Symposium, 2010 IEEE*, March 2010, pp. 141–148.

[16] J. Romano and K. Kuchenbecker, "Creating realistic virtual textures from contact acceleration data," *Haptics, IEEE Transactions on*, vol. 5, no. 2, pp. 109–119, April 2012.

[17] M. A. Costa and M. R. Cutkosky, "Roughness perception of haptically displayed fractal surfaces," in *Proceedings of the ASME dynamic systems and control division*, vol. 69, no. 2, 2000, pp. 1073–1079.

[18] S. A. Wall and W. S. Harwin, "Modelling of surface identifying characteristics using fourier series," *ASME DYN SYST CONTROL DIV PUBL DSC.*, vol. 67, pp. 65–71, 1999.

[19] M. Minsky, "Simulated haptic textures: Roughness," 1996.

[20] K.-U. Kyung and J.-Y. Lee, "Ubi-pen: a haptic interface with texture and vibrotactile display." *IEEE Computer Graphics and Applications*, vol. 29, no. 1, pp. 56–64, 2008.

[21] D. A. Kontarinis and R. D. Howe, "Tactile display of vibratory information in teleoperation and virtual environments," *Presence*, vol. 4, pp. 387–402, 1996.

[22] K. J. Kuchenbecker, J. Gewirtz, W. McMahan, D. Standish, P. Martin, J. Bohren, P. J. Mendoza, and D. I. Lee, "Verrotouch: high-frequency acceleration feedback for telerobotic surgery," in *Haptics: Generating and Perceiving Tangible Sensations*. Springer, 2010, pp. 189–196.

[23] J. M. Romano and K. J. Kuchenbecker, "Creating realistic virtual textures from contact acceleration data," *Haptics, IEEE Transactions on*, vol. 5, no. 2, pp. 109–119, 2012.

[24] A. Yamamoto, S. Nagasawa, H. Yamamoto, and T. Higuchi, "Electrostatic tactile display with thin film slider and its application to tactile telepresentation systems," *Visualization and Computer Graphics, IEEE Transactions on*, vol. 12, no. 2, pp. 168–177, 2006.

[25] M. Wiertlewski, D. Leonardis, D. Meyer, M. Peshkin, and J. Colgate, "A high-fidelity surface-haptic device for texture rendering on bare finger," in *Haptics: Neuroscience, Devices, Modeling, and Applications*, ser. Lecture Notes in Computer Science, M. Auvray and C. Duriez, Eds. Springer Berlin Heidelberg, 2014, pp. 241–248.

[26] K. Minamizawa, H. Kajimoto, N. Kawakami, and S. Tachi, "A wearable haptic display to present the gravity sensation - preliminary observations and device design," in *EuroHaptics Conference, 2007 and Symposium on Haptic Interfaces for Virtual Environment and Teleoperator Systems. World Haptics 2007. Second Joint*, March 2007, pp. 133–138.

[27] J. C. Gwilliam, M. Bianchi, L. K. Su, and A. M. Okamura, "Characterization and psychophysical studies of an air-jet lump display," *Haptics, IEEE Transactions on*, vol. 6, no. 2, pp. 156–166, 2013.

[28] K. J. Waldron, C. Enedah, and H. Gladstone, "Stiffness and texture perception for teledermatology," *Studies in health technology and informatics*, vol. 111, pp. 579–585, 2005.

[29] M. Bianchi, E. Scilingo, A. Serio, and A. Bicchi, "A new softness display based on bi-elastic fabric," in *EuroHaptics conference, 2009 and Symposium on Haptic Interfaces for Virtual Environment and Teleoperator Systems. World Haptics 2009. Third Joint*, March 2009, pp. 382–383.

[30] S. J. Lederman and R. L. Klatzky, "Hand movements: A window into haptic object recognition," *Cognitive psychology*, vol. 19, no. 3, pp. 342–368, 1987.

[31] ——, "Haptic classification of common objects: Knowledge-driven exploration," *Cognitive psychology*, vol. 22, no. 4, pp. 421–459, 1990.

[32] J. Bell, S. Bolanowski, and M. H. Holmes, "The structure and function of pacinian corpuscles: A review," *Progress in neurobiology*, vol. 42, no. 1, pp. 79–128, 1994.

[33] N. Landin, J. M. Romano, W. McMahan, and K. J. Kuchenbecker, "Dimensional reduction of high-frequency accelerations for haptic rendering," in *Haptics: Generating and Perceiving Tangible Sensations, Proc. EuroHaptics, Part II*, ser. Lecture Notes in Computer Science, A. M. L. Kappers, J. B. F. van Erp, W. M. B. Tiest, and F. C. T. van der Helm, Eds., vol. 6192. Springer, July 2010, pp. 79–86.

[34] H. Culbertson, J. M. Romano, P. Castillo, M. Mintz, and K. J. Kuchenbecker, "Refined methods for creating realistic haptic virtual textures from tool-mediated contact acceleration data," in *Haptics Symposium (HAPTICS), 2012 IEEE*. IEEE, 2012, pp. 385–391.